SCIENTIFIC REPORTS

Correspondence and
requests for materials
should be addressed to
H.-Y.H. (hyhu@sibcb.
ac.cn)

Aggregation of polyglutamine-expanded ataxin-3 sequesters its specific interacting partners into inclusions: Implication in a loss-of-function pathology

Hui Yang, Jing-Jing Li, Shuai Liu, Jian Zhao, Ya-Jun Jiang, Ai-Xin Song & Hong-Yu Hu

State Key Laboratory of Molecular Biology, Institute of Biochemistry and Cell Biology, Shanghai Institutes for Biological Sciences, Chinese Academy of Sciences. 320 Yue-Yang Road, Shanghai 200031, China.

Expansion of polyglutamine (polyQ) tract may cause protein misfolding and aggregation that lead to cytotoxicity and neurodegeneration, but the underlying mechanism remains to be elucidated. We applied ataxin-3 (Atx3), a polyQ tract-containing protein, as a model to study sequestration of normal cellular proteins. We found that the aggregates formed by polyQ-expanded Atx3 sequester its interacting partners, such as P97/VCP and ubiquitin conjugates, into the protein inclusions through specific interactions both *in vitro* and in cells. Moreover, this specific sequestration impairs the normal cellular function of P97 in down-regulating neddylation. However, expansion of polyQ tract in Atx3 does not alter the conformation of its surrounding regions and the interaction affinities with the interacting partners, although it indeed facilitates misfolding and aggregation of the Atx3 protein. Thus, we propose a loss-of-function pathology for polyQ diseases that sequestration of the cellular essential proteins via specific interactions into inclusions by the polyQ aggregates causes dysfunction of the corresponding proteins, and consequently leads to neurodegeneration.

P rotein misfolding often results in aberrant formation of insoluble aggregates or inclusion bodies, which are strongly associated with the pathogenesis of some neurodegenerative diseases[1]. Polyglutamine (polyQ) diseases are a group of ten genetic diseases that are caused by expansion of the polyQ tract in the corresponding proteins[2–4]. Previous studies reported that polyQ expansion of the disease proteins tend to induce misfolding and aggregation due to a conformational change within the proteins[5,6]. A hypothesis states that formation of inclusions is one of the cellular protective processes to resist the toxicities of the soluble oligomers of the misfolded disease proteins[7,8]. However, there are some studies suggesting that the insoluble aggregates or inclusions are able to sequester normal cellular proteins into the inclusions and cause dysfunction of these essential proteins[9–16]. These experimental data support an assumption that more and more cellular proteins are sequestered into insoluble aggregates or inclusions that cause them dysfunctional and cytotoxic.

Although accumulating studies have approached to the pathogenesis of polyQ diseases, many important problems still remain to be solved. For example, whether a polyQ protein sequesters cellular proteins through specific or non-specific interactions has not been clearly understood. It is still controversial whether polyQ expansion affects the protein conformation and interactions with other proteins. And finally, whether the cytotoxicity of polyQ-protein inclusions is resulted from sequestration of the cellular essential proteins needs more experimental evidence.

We applied ataxin-3 (Atx3), a polyQ tract-containing protein related to spinocerebellar ataxia type-3 (SCA3) disease, as a model molecule to address these puzzles. Atx3 is a deubiquitinating enzyme that functions in ubiquitin (Ub)-proteasome pathway[17,18] and endoplasmic reticulum-associated degradation (ERAD)[19–21]. Besides, it has two alternatively spliced isoforms with distinct C-termini[22,23] (See Fig. 1a). Isoform I (Atx3-I) contains two tandem Ub-interacting motifs (UIMs), whereas isoform II (Atx3-II) has an additional UIM following the polyQ tract and it is predominant in brain that may contribute to the selective neurotoxicity[24]. The UIM motifs bind Ub chains, which is responsible for the substrate presentation[17,23,25]. Atx3 prossesses a Josephin domain in the N-terminus[26], which mediates the deubiquitinating enzyme activity[27]. Moreover, Atx3 interacts with P97/VCP through a VCP-binding motif (VBM)[28,29]. Following the VBM motif is a polyQ tract with variable
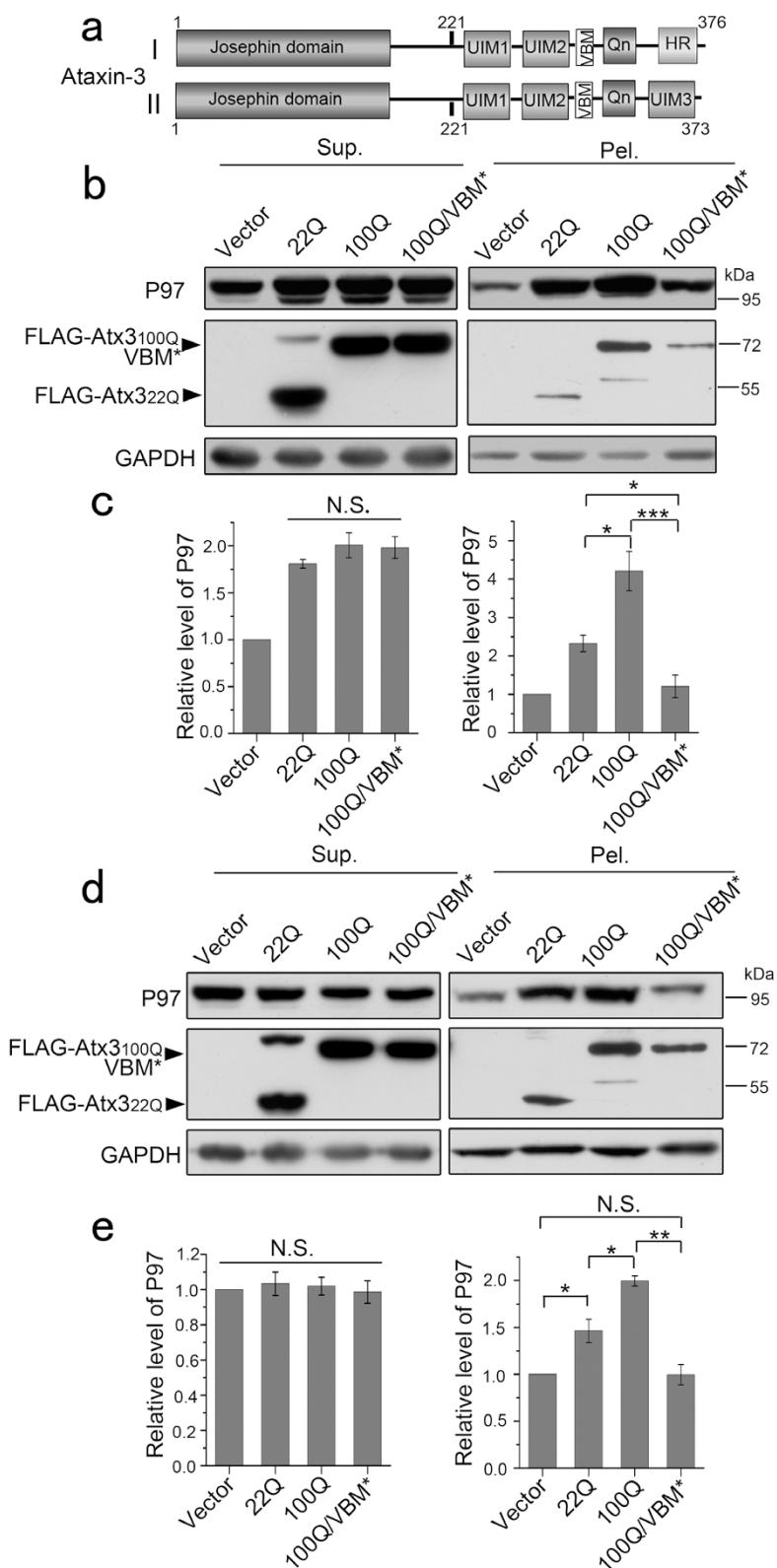
Figure 1 | Sequestration of P97 into insoluble aggregates by Atx3. (a) Domain architecture of the two isoforms of Atx3. Josephin domain, a deubiquitinating domain of Atx3; UIM, ubiquitin-interacting motif; VBM, VCP-binding motif; HR, hydrophobic region; Qn, polyQ tract. The expanded glutamine residues are not included in the numbering. (b) Sequestration of overexpressed P97. FLAG-tagged $Atx3_{22Q}$, $Atx3_{100Q}$ or $Atx3_{100Q}$/VBM* (^{282}RKRR to HNHH) was co-transfected with HA-P97 into HEK 293T cells. The cell lysates were subjected to fractionation and Western blotting with an anti-FLAG or anti-HA antibody. The constructs contain sequences encoding the amino-acid residues of 1 - 360. Sup., supernatant; Pel., pellet. (c) Quantification of the amounts of overexpressed HA-P97 in supernatant and pellet fractions. (d) Sequestration of endogenous P97. FLAG-tagged $Atx3_{22Q}$, $Atx3_{100Q}$ or $Atx3_{100Q}$/VBM* was transfected into HEK 293T cells. The cell lysates were subjected to fractionation and Western blotting with an antibody against P97. (e) Quantification of the amounts of endogenous P97 in supernatant and pellet fractions. Data are shown as Means $\pm$ SEM (n = 3). *, p < 0.05; **, p < 0.01; ***, p < 0.001; N.S., no significance.

length, which is thought to be associated with the SCA3 disease[3,30]. The polyQ-expanded Atx3 is prone to aggregation and inclusion formation in the neurons of patients with SCA3 disease[31–33].

We investigated how polyQ-expanded Atx3 sequesters its associated proteins and influences their functions by biochemical and biophysical approaches. We found that the aggregates formed by polyQ-expanded Atx3 sequester cellular P97 and Ub conjugates through specific interactions, and this specific sequestration interferes with the function of P97 in down-regulating neddylation in cells. The snowball-like sequestration of cellular essential proteins by polyQ aggregates was proposed to be associated with the cytotoxicity and neurodegeneration.

Results

PolyQ-expanded Atx3 sequesters P97 to aggregates through specific interaction. It was previously reported that the inclusions formed by Atx3 contain many other proteins, including molecular chaperones, Ub-proteasome components, P97 and P62/SQSTM1, and these hijacked proteins are involved in the toxicity of polyQ-expanded Atx3[28,31,34–36]. However, whether the sequestrations are caused by specific interactions remains elusive. Because Atx3 binds P97 through a VBM motif[28], we applied isoform I of Atx3 (Atx3-I) as a molecular model to explore the relationship between sequestration and specific interaction (Fig. 1a). We co-transfected HA-P97 and various FLAG-tagged Atx3 forms ($Atx3_{22Q}$, $Atx3_{100Q}$ or its mutant) respectively into HEK 293T cells and performed supernatant-pellet fractionation (Fig. 1b). The result showed that most $Atx3_{22Q}$ remained in the supernatant; whereas an increased fraction of $Atx3_{100Q}$ was accumulated in the aggregate form. When P97 was co-expressed with any type of Atx3, its amounts in supernatant exhibited a slight increase as compared with that of the negative control, but they were no significant difference (Fig. 1b & 1c, left). However, in the pellet fractions, $Atx3_{100Q}$ sequestered more P97 molecules into aggregates than $Atx3_{22Q}$, due to an increasing amount of $Atx3_{100Q}$ in the pellet (Fig. 1b & 1c, right). Interestingly, mutation in the VBM motif of $Atx3_{100Q}$ ($Atx3_{100Q}$/VBM*, [282]RKRR to HNHH), which disrupts the specific interaction between Atx3 and P97, significantly abolished the sequestration of P97 into aggregates; even the amount of P97 sequestered by the mutant was less than that by $Atx3_{22Q}$ under the condition of similar amounts of the Atx3 aggregates (Fig. 1b & 1c, right). It should be mentioned that the insoluble aggregates formed by the VBM mutant were less than those by the wild-type $Atx3_{100Q}$. So we carried out immunofluorescence microscopic imaging of the three forms in cells (Supplementary Fig. S1). The data showed that the VBM motif did not overlap with the nuclear localization signal region of Atx3[37,38], excluding the possibility that the reduced insoluble aggregates are caused by the subcellular distribution change. We also applied filter-trap assay to detect the aggregates formed by these three Atx3 species. Indeed, the SDS-insoluble aggregates formed by the mutant were considerably less than those by the wild-type (Supplementary Fig. S2). Although it cannot be excluded that the lower amount of the aggregates may have some correlation to the decreased sequestration, we think that the major contribution to the decreased ability of the VBM mutant to sequester P97 is from disruption of the specific interaction between $Atx3_{100Q}$ and P97.

To better understand the aggregation effects of polyQ-expanded Atx3, we further examined whether $Atx3_{100Q}$ redistributes endogenous P97 in cells. When the three Atx3 forms were overexpressed as above, similar amounts of the endogenous P97 in the supernatant fraction were observed (Fig. 1d & 1e, left). However, aggregation of $Atx3_{100Q}$ could sequester more endogenous P97 than that of $Atx3_{22Q}$ (Fig. 1d & 1e, right). Moreover, the VBM mutation of $Atx3_{100Q}$ abolished this co-precipitation effect. Even the amount of endogenous P97 co-precipitated by the $Atx3_{100Q}$ mutant was less than that by wild-type $Atx3_{22Q}$ in the pellet fraction. These results demonstrate

that polyQ-expanded Atx3 sequesters P97 molecules into insoluble aggregates or inclusions, which is dependent on the specific interaction via the VBM motif of Atx3.

PolyQ-expanded Atx3 influences the function of P97 in down-regulating neddylation in cells. Because polyQ-expanded Atx3 can sequester endogenous P97 into insoluble aggregates, we resorted to the previously established experiment to explore whether aggregation of Atx3 interferes with the function of P97. As reported, P97 down-regulates the neddylation in cells, and knock-down of endogenous P97 increases the protein level of NEDD8 conjugates[39]. We performed co-transfection of HA-NEDD8 and the indicated forms of Atx3 respectively into HEK 293T cells, and detected the neddylation levels by Western blotting. The result showed that overexpression of $Atx3_{100Q}$ significantly increased the level of neddylation compared to those of $Atx3_{22Q}$ and $Atx3_{100Q}$/VBM* (Fig. 2a, 2b). It was reported that Atx3 interacts with NEDD8 via its Josephin domain (Fig. 1a), and displays deneddylase activity *in vitro*[40]. To rule out the possible interference of deneddylation, we prepared the C-terminal fragments of Atx3-I with deletion of the Josephin domain (Atx3-IC, residues 221–360) and repeated the above experiment. Similarly, overexpression of $Atx3_{100Q}$-IC still significantly increased the neddylation level as compared with those of $Atx3_{22Q}$-IC and $Atx3_{100Q}$-IC/VBM* (Fig. 2c, 2d). It implies that polyQ-expanded Atx3 impairs the function of P97 complex that is capable of down-regulating the neddylation level in cells. In addition, there was no significant difference of the neddylation levels between $Atx3_{100Q}$/VBM* and $Atx3_{22Q}$ (Fig. 2b), as well as the $Atx3_{100Q}$-IC/VBM* and $Atx3_{22Q}$-IC cases (Fig. 2d). It suggests that aggregation of polyQ-expanded Atx3 interferes with the normal function of P97 in down-regulating neddylation depending on the specific interaction through VBM. This finding is conflicting with the previous viewpoint that the polyQ tracts mediate the interactions between P97 and the polyQ proteins and subsequently affect the function of P97[16].

PolyQ-expanded Atx3 sequesters Ub conjugates into aggregates. It is reported that inclusions of polyQ-expanded Atx3 is Ub-positive[13,31]. We next investigated whether polyQ-expanded Atx3 sequesters Ub conjugates into insoluble aggregates. Due to the Josephin domain also possesses Ub-interaction and deubiquitination properties[41], for simplicity, we applied the C-terminal fragments of Atx3-I (Atx3-IC) comprised of two UIMs and the polyQ tract as a model for the studies. Note that the C-terminal fragments of polyQ-expanded Atx3 are also implicated in the disease pathology[38,42,43]. The experimental data showed that $Atx3_{100Q}$-IC sequestered more amount of ubiquitinated proteins, both in overexpressed (Fig. 3a) and endogenous Ub forms (Fig. 3b), into insoluble aggregates than $Atx3_{22Q}$-IC, whereas the levels of Ub conjugates retained in the supernatant fraction were roughly invariant. However, the UIM mutant ($Atx3_{100Q}$-IC/UIM*, S236A/S256A) sequestered less amount of ubiquitinated proteins into aggregates than $Atx3_{100Q}$-IC. As known, substitution of the conserved serine residues with alanine in the UIM region nearly disrupts the interaction between Atx3 and ubiquitinated proteins[23]. This demonstrates that polyQ-expanded Atx3 sequesters Ub conjugates into insoluble aggregates depending on specific interactions via the UIM motifs of Atx3.

PolyQ-expanded Atx3 sequesters its interacting partners into insoluble aggregates *in vitro*. To corroborate the above observation, we investigated the sequestration effect of polyQ-expanded Atx3 on its interacting partners *in vitro*. We purified the C-terminal part of isoform II Atx3 (Atx3-IIC, residues 221–373) with different polyQ lengths (6Q, 22Q and 46Q) (Supplementary Fig. S3). Size exclusion chromatography (SEC) showed that the wild-type $Atx3_{22Q}$-IIC and polyQ-truncated $Atx3_{6Q}$-IIC were rather stable in solution, but the polyQ-expanded $Atx3_{46Q}$-IIC readily formed oligomers or was susceptible to degradation (Supplementary Fig. S4)[44]. We then
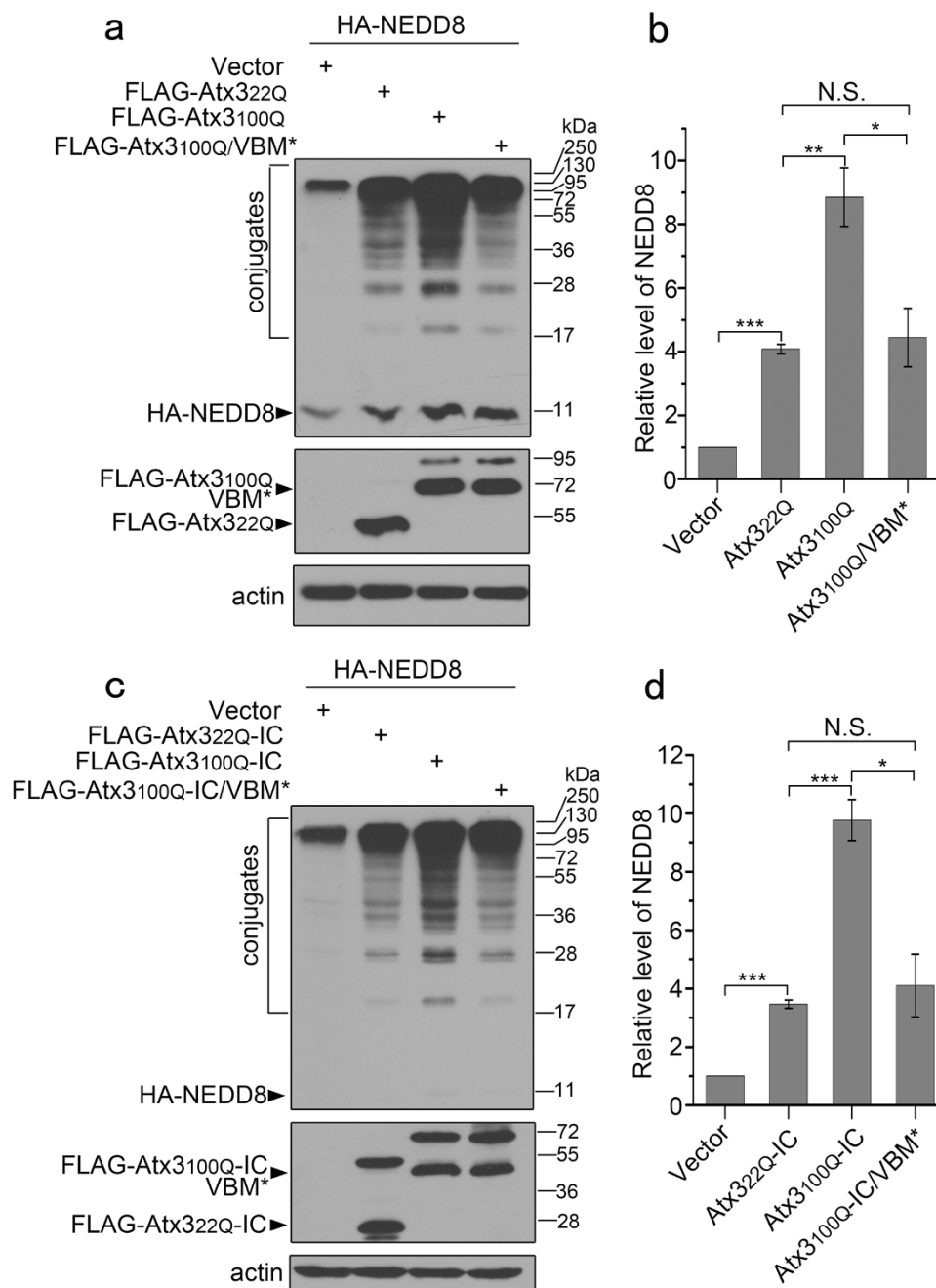
Figure 2 | Effect of polyQ-expanded Atx3 on the function of P97 in down-regulating neddylation. (a) Effect of polyQ-expanded Atx3 on the neddylation levels in cells. HEK 293T cells were co-transfected with HA-NEDD8 and FLAG-tagged Atx3$_{22Q}$, Atx3$_{100Q}$ or Atx3$_{100Q}$/VBM*. About 72 hrs after transfection, the cell lysates were prepared for Western blotting with an anti-FLAG or anti-HA antibody. (b) Quantification of the neddylation levels by three Atx3 types. (c) Effect of polyQ-expanded Atx3-IC on the neddylation levels in cells. Same as (a), but the C-terminal fragments of Atx3 (residues 221–360; Atx3$_{22Q}$-IC, Atx3$_{100Q}$-IC or Atx3$_{100Q}$-IC/VBM*) applied. (d) Quantification of the neddylation levels by the three Atx3-IC forms. Data are shown as Means ± SEM (n = 4). *, p < 0.05; **, p < 0.01; ***, p < 0.001; N.S., no significance.

performed fractionation analysis on the incubation mixtures of Atx3-IIC and K48-diUb (Lys48-linked di-ubiquitin) or P97-ND1 (residues 1–458, a fragment of P97 with N and D1 domains)[29] by separating the supernatant and pellet fractions from the aggregated proteins (Fig. 4). After incubation for 48 hrs, most of the Atx3$_{22Q}$-IIC protein remained in the supernatant fraction, while a large part of Atx3$_{46Q}$-IIC precipitated into the pellet. Interestingly, the Atx3$_{46Q}$-IIC aggregates could hijack K48-diUb (Fig. 4b) and P97-ND1 (Fig. 4d) into the pellet fractions in a dose-dependent manner. As a control, thioredoxin (Trx) could not be co-precipitated by the Atx3$_{46Q}$-IIC aggregates (Supplementary Fig. S5). Thus, the insoluble aggregates formed by Atx3$_{46Q}$-

IIC can sequester its interacting partners K48-diUb and P97 *in vitro*, further demonstrating that specific interaction is crucial to the protein sequestration.

PolyQ expansion in Atx3 has little effect on its interacting affinities with partners and the surrounding conformations. There are many literatures reporting that polyQ expansion is responsible for enhancing the interaction with the partners and sequestration of them[9,16]. To clarify whether polyQ tract has notable effect on the interactions with its partners, we measured the binding affinities of these three Atx3-IIC forms with K48-diUb or P97 by isothermal
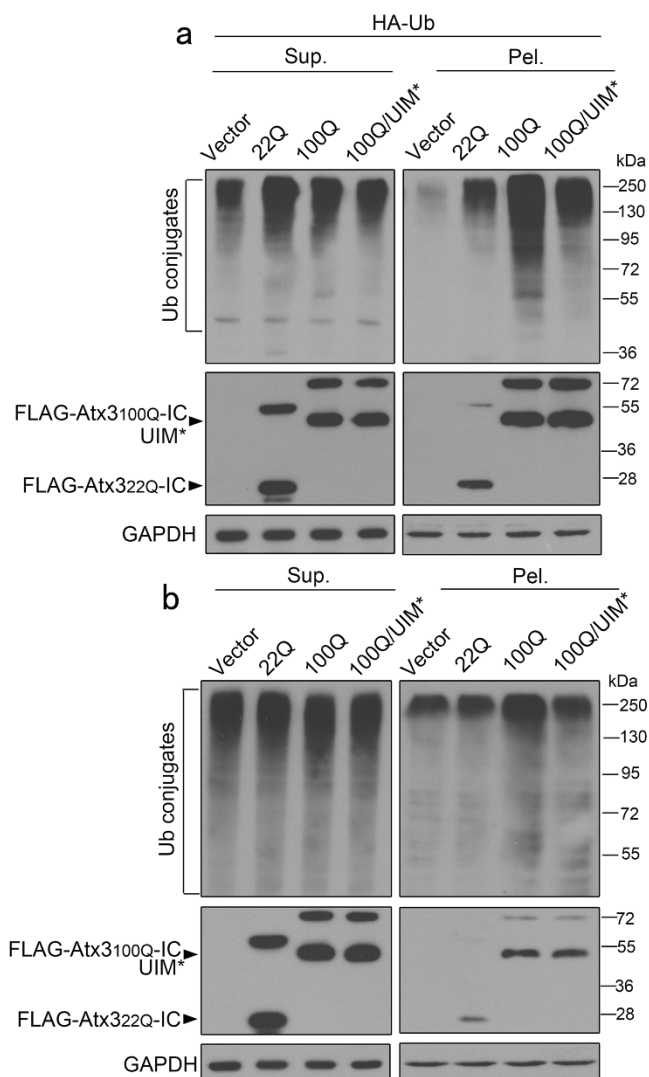
Figure 3 | Sequestration of the ubiquitin conjugates into insoluble aggregates by Atx3. (a) Sequestration of overexpressed Ub conjugates. FLAG-tagged Atx3$_{22Q}$-IC, Atx3$_{100Q}$-IC or Atx3$_{100Q}$-IC/UIM* was co-transfected with HA-Ub into HEK 293T cells. The cell lysates were subjected to fractionation and Western blotting with an anti-FLAG or anti-HA antibody. (b) Sequestration of endogenous Ub conjugates. FLAG-tagged Atx3$_{22Q}$-IC, Atx3$_{100Q}$-IC or Atx3$_{100Q}$-IC/UIM* was transfected into HEK 293T cells. The cell lysates were subjected to fractionation and Western blotting with an antibody against Ub. Sup., supernatant; Pel., pellet. Atx3-IC, C-terminal fragment (residues 221–360) of isoform-I Atx3; UIM*, mutation in UIM domain, S236A/S256A.

titration calorimetry (ITC) experiments. The data showed that three forms of Atx3-IIC interacted with K48-diUb with similar affinities, which were around 50 μM (Fig. 5a), indicating that the interactions of Atx3-IIC with different polyQ lengths exhibit similar affinities with K48-diUb. We also purified the N-terminal domain of P97 (residues 1–213, P97N)[29], which is potent to interact with various VBM motifs[28]. The ITC data also re-confirmed that all the Atx3-IIC forms bound P97N with similar affinities around 10 μM (Fig. 5b). This is consistent with the results from Atx3 and huntingtin (Htt) that their affinities with the interacting partners are not changed by polyQ expansion[17,45]. Thus, we conclude that the polyQ tract, no matter elongation or truncation, has no significant impact on the interactions of Atx3-IIC with K48-diUb and P97.

It is known that polyQ tract adopts β-sheet structures during aggregation, but whether polyQ expansion influences its surround-

ing conformation is unclear[46–48]. To address this issue, we investigated the potential effect of polyQ-tract length on the conformation of Atx3 by NMR (Supplementary Fig. S6). We compared the ^{1}H-^{15}N HSQC spectra of these Atx3-IIC forms. The resonance peaks of Atx3$_{6Q}$-IIC (Fig. 5c) or Atx3$_{46Q}$-IIC (Fig. 5d) could overlap with those of Atx3$_{22Q}$-IIC, suggesting that truncation or elongation of the polyQ tract has little effect on their overall conformations especially those of the flanking UIM and VBM motifs. This is inconsistent with the previous viewpoint that polyQ expansion could alter the conformations of the surrounding regions[49]. Taken together, polyQ expansion has little effect on the conformation of Atx3 and the interaction with its partners, whereas aggregation of Atx3 caused by polyQ expansion is the prerequisite for sequestering or hijacking its interacting partners.

Discussion

PolyQ-protein aggregates hijack cellular essential proteins. The polyQ expansion above a threshold of certain length results in abnormal aggregation and inclusion formation, which may have toxic effect on the patient brains and lead to the neurodegenerative diseases[3]. We have found that aggregation of polyQ-expanded Atx3 can sequester P97 and Ub conjugates into the protein aggregates or inclusions through specific interactions both *in vitro* and in cells. The sequestration also impairs the normal cellular function of P97 in down-regulating neddylation. As known, the polyQ proteins that contain other domains and/or motifs besides the polyQ tracts have potential to specifically interacting with its partners in solution. Expansion of polyQ may cause protein misfolding and formation of insoluble aggregates or inclusions, which are able to co-precipitate or sequester their interacting partners into insolubilities (Fig. 6). This snowball-like sequestration effect may cause some related proteins dysfunctional and cytotoxic[50].

Protein sequestration mediated by specific interaction. A number of literatures report that sequestration of other cellular proteins by protein interactions or associations[9–12,15]. Molecular chaperones (such as HSP70 and HSP90) and ubiquitin-proteasome components are often considered to be hijacked by polyQ-expanded aggregates by non-specific sequestration (here referred to as adsorption)[13,14,16]. This is probably due to the fact that the cellular quality-control system is aimed to resist the misfolding and aggregation of polyQ-expanded proteins. For example, P97 was previously reported to directly interact with the polyQ tracts of several proteins and these interactions might impair normal function of the P97 complex[16]. This might just be the indirect protein association or adsorption due to involvement of P97 in quality control, because sequestration of P97 by polyQ-expanded Atx1 or Htt is non-specific. Our studies have revealed that P97 and Ub conjugates are sequestered by polyQ-expanded Atx3 through specific interactions in cells, and this is also confirmed by *in vitro* experiments. These specific interactions are mediated by particular domains or motifs; mutation of these regions may disrupt the interactions and then abolish their sequestration effects. In this situation, it could be referred to as specific sequestration, being distinct from the non-specific association or adsorption.

PolyQ expansion may induce misfolding of the disease protein to adopt a high content of β-sheet conformation[51], which leads to formation of amyloid-like protein aggregates[52,53]. We and Fujita et al. have observed by co-immunoprecipitation that polyQ expansion enhances the association affinities of polyQ proteins, such as Htt with HYPA[9] or P97[16]. However, inconsistent with Fujita et al.[16], we hold that polyQ is not directly involved in interaction with the partners, but it contributes to misfolding and aggregation. Therefore, it is rational to deduce that polyQ expansion significantly alters the affinities with other interacting partners due to a phase transition from soluble monomers to oligomers and to insoluble aggregates. In light
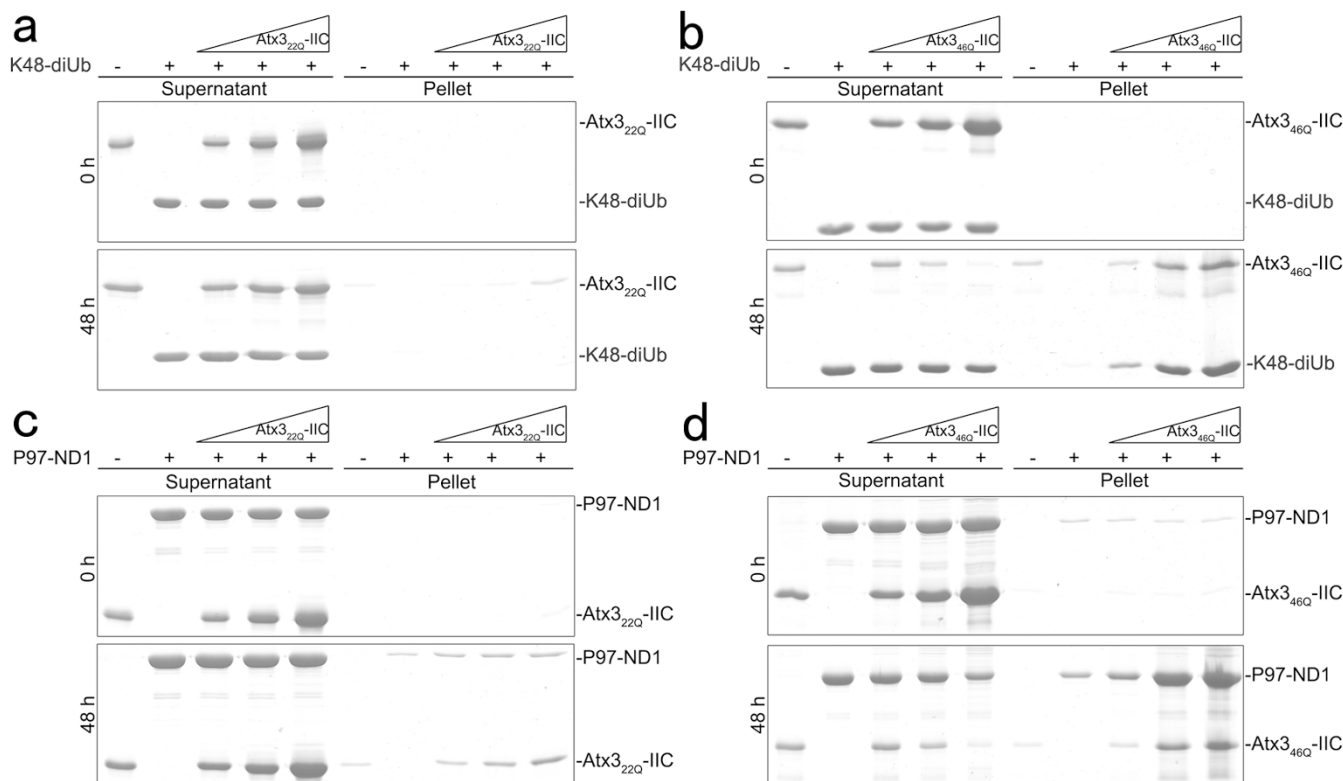
Figure 4 | Co-precipitation of diUb and P97 by Atx3 as detected by fractionation and SDS-PAGE analysis. (a) K48-diUb by $Atx3_{22Q}$-IIC. (b) K48-diUb by $Atx3_{46Q}$-IIC. (c) P97-ND1 by $Atx3_{22Q}$-IIC. (d) P97-ND1 by $Atx3_{46Q}$-IIC. The protein mixtures were centrifuged to separate supernatant (Sup.) and pellet (Pel.), and analyzed by SDS-PAGE (15% gel). The stock concentrations of $Atx3_{22Q}$-IIC and $Atx3_{46Q}$-IIC were 600 µM. $Atx3_{22Q}$-IIC or $Atx3_{46Q}$-IIC was mixed with K48-diUb (60 µM) at an increased molar ratio of Atx3-IIC/K48-diUb (0 : 1, 1.5 : 1, 3 : 1 and 6 : 1), while it was mixed with P97-ND1 (30 µM) at an increased molar ratio (0 : 1, 3 : 1, 6 : 1 and 12 : 1). Atx3-IIC, C-terminal fragment (residues 221–373) of isoform-II Atx3. K48-diUb, K48-linked diubiquitin.

of these, we speculate that the direct effect of polyQ expansion is to entice the protein prone to aggregation, which, during aggregating process, alters its state from soluble to insoluble and simultaneously sequesters its interacting partners into the insolubilities.

Specific protein sequestration implicated in a loss-of-function pathology. It is possible that either soluble oligomers or fibrillar aggregates formed by polyQ-expanded proteins are associated with the neurotoxicities in polyQ diseases[8,54], but the pathogenic mechanism by which polyQ-expanded protein causes cytotoxicity and neurodegeneration remain largely unknown. P97 is a key protein involved in various cellular functions including ERAD[55], DNA double-stranded break repair[56], neddylation regulation[39], and so on. We have revealed that polyQ-expanded Atx3 can significantly interfere with the normal function of P97 in down-regulating neddylation by specific protein sequestration (Fig. 2), implying that sequestration of the key protein P97 by the Atx3 aggregates can induce cellular dysfunction. We speculate that sequestration of cellular essential proteins by polyQ aggregates, regardless through specific or non-specific interaction, leads to cellular loss-of-function and toxic effects and even causes cell death. Therefore, sequestration of the cellular essential proteins by protein aggregates might be one of the pathological sources of cytotoxicity and neurodegeneration.

Methods

Plasmids, antibodies and reagents. For eukaryotic expression, Atx3-I, Atx3-IC and their mutants were cloned into a FLAG-pcDNA3.0 vector, while P97, Ub and NEDD8 were cloned into HA pcDNA3.0. For prokaryotic expression, the C-terminal fragments of Atx3-II (22Q, 6Q) were cloned into pET-22b(+), while $Atx3_{46Q}$-IIC was cloned into pGBTNH, which encodes the fusion protein with a GB1 domain in the N terminus[57]. P97-ND1 (residues 1–458) and P97N (1–213) were cloned into pET-22b(+), while Ub was cloned into pET-3a. The anti-FLAG antibody was from Sigma;

anti-HA, anti-Ub and anti-actin were from Santa Cruz; and anti-GAPDH was from Zen BioScience. All the secondary antibodies were purchased from Jackson Immuno-Research. PVDF membranes were obtained from PerkinElmer Life Sciences, and ECL detection kit for proteins was from Thermoscientific.

Protein expression and purification. All the proteins were overexpressed in E. coli BL21 (DE3) strain (Invitrogen). ^{15}N and^{15}N/^{13}C-labeled Atx3-IIC proteins were overexpressed in M9 minimal media using [^{15}N]-NH$_4$Cl and/or [^{13}C]-glucose as the sole nitrogen and carbon sources (Cambridge Isotope Laboratories). The His-tag fused proteins were initially purified by a Ni^{2+}-NTA column (Qiagen), followed by size-exclusion chromatography (Superdex-75 or Superdex-200, GE Healthcare). After the GB1-fused $Atx3_{46Q}$-IIC was eluted from Ni^{2+}-NTA column, the GB1 tag was removed by thrombin digestion followed by a second Ni^{2+}-NTA column and a Superdex-200 column. The resulting peptide fragments contain two extra residues, Gly and Ser, at the N-terminus and a His6 tag at the C-terminus. Ub was purified by cation exchange column (HiPrep 16/10 SP XL, GE Healthcare), followed by size-exclusion chromatography (Superdex-75, GE Healthcare). Purified Ub was dialyzed against water, lyophilized and stored at −20°C. The K48-diUb was prepared according to the literatures[58,59].

Fractionation of supernatant and pellet. HEK 293T cells were cultured in Dulbecco's modified Eagle's medium (DMEM) (Invitrogen) supplemented with 10% fetal bovine serum (Gibco) and penicillin and streptomycin at 37°C under a humidified atmosphere containing 5% CO$_2$. All transfections were performed by using PolyJet™ (SignaGen) reagent. Cells transfected with specific plasmids were lysed in100 µL of RIPA buffer (50 mM Tris-HCl, pH 7.5, 150 mM NaCl, 1 mM EDTA, 1% NP-40, cocktail protease inhibitor (Roche Applied Science)) on ice for 0.5 hr and centrifuged at 16,200 g for 15 min. The supernatant was added with 100 µL of the loading buffer (2% SDS), while the pellet was sufficiently washed with RIPA buffer for three times and then added with 30 µL of the loading buffer (4% SDS).

***In vitro* co-precipitation experiments.** The co-precipitation experiments were performed in a PBS buffer (140 mM NaCl, 2.7 mM KCl, 10 mM Na$_2$HPO$_4$, 1.8 mM KH$_2$PO$_4$, pH 7.3). The stock concentrations of $Atx3_{22Q}$-IIC and $Atx3_{46Q}$-IIC were 600 µM. The Atx3-IIC protein was mixed with K48-diUb or P97-ND1 at an increased molar ratio. The protein mixtures were incubated at room temperature for 48 hrs.
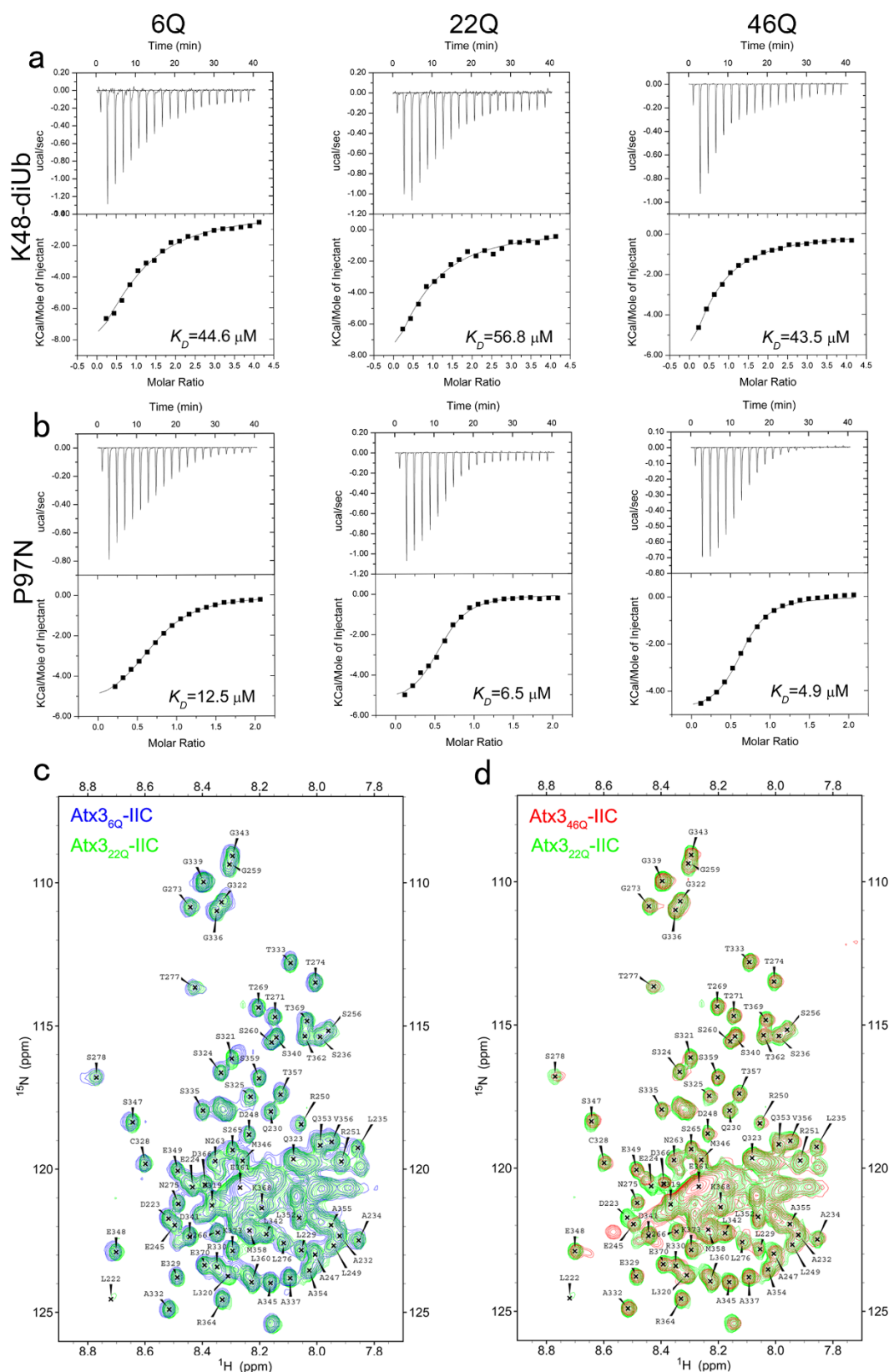
Figure 5 | Characterization of the effects of polyQ expansion in Atx3 on its interacting affinities with partners and the surrounding conformations.
(a, b) Determining the interaction affinities of three Atx3 forms with K48-diUb (a) and P97N (b) by ITC experiments. The three Atx3 forms were Atx3$_{6Q}$-IIC, Atx3$_{22Q}$-IIC and Atx3$_{46Q}$-IIC, respectively. The binding constants were calculated by fitting the ITC data with one-site model. The concentrations of Atx3-IIC forms were 50 μM, while those of K48-diUb and P97N stocks were ~1 mM. (c, d) Detecting the effect of polyQ tract on the surrounding conformations of Atx3 by NMR. (c) Overlay of the ^{1}H-^{15}N HSQC spectra of Atx3$_{22Q}$-IIC (green) and Atx3$_{6Q}$-IIC (blue). (d) Overlay of the ^{1}H-^{15}N HSQC spectra of Atx3$_{22Q}$-IIC (green) and Atx3$_{46Q}$-IIC (red). The concentration of each protein was ~150 μM. The non-overlapped resonance peak (red) denotes the N-terminally additional residue of Atx3$_{46Q}$-IIC.
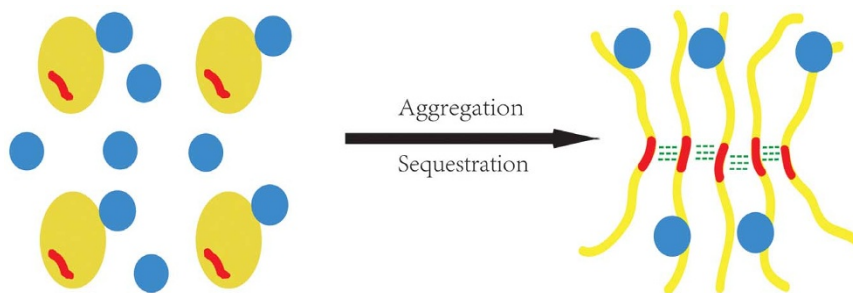
Figure 6 | Schematic model for polyQ aggregates hijacking the specific interacting partners. The polyQ protein is shown in yellow, while the interacting protein is in blue. The polyQ tract is highlighted in red.

The supernatant and pellet were separated via centrifuging the 20-μL sample with 13,000 rpm at 4°C for 20 min. Then the supernatant and pellet fractions were subjected to SDS-PAGE (15% gel), followed by Coomassie blue staining.

Isothermal titration calorimetry (ITC). The ITC experiments were performed on a MicroCal iTC200 at 25°C in an ITC buffer (20 mM Tris-Cl, 50 mM NaCl, pH 7.5). The K48-diUb or p97/VCP protein (1 mM) stocked in a syringe was injected into a 300-μL sample of $Atx3_{6Q}$-IIC (50 μM), $Atx3_{22Q}$-IIC (50 μM) or $Atx3_{46Q}$-IIC (50 μM). The binding constants were calculated by fitting the data with one-site binding model using Origin 7.0 software (OriginLab Corp.).

Nuclear magnetic resonance (NMR) spectroscopy. The NMR experiments were carried out at 25°C on a Bruker Avance III 600-MHz spectrometer equipped with four RF channels and a triple-resonance pulsed-field gradient probe. The samples were prepared with 1 mM protein dissolved in 90% H_2O/10% D_2O buffer containing 20 mM sodium phosphate (pH 6.5), 50 mM NaCl, and 1 mM DTT. Three-dimensional CBCA(CO)NH, HNCACB, HNCO, (H)CC(CO)NH TOCSY experiments were performed to obtain the chemical-shift assignments of the backbone atoms[25]. The titration experiments of $Atx3_{22Q}$-IIC with K48-diUb were monitored by a series of two-dimensional ^1H-^{15}N HSQC spectra[60]. During the titration, the molar ratios of K48-diUb/$Atx3_{22Q}$-IIC were increased from 0.25 : 1 to 2 : 1.

1. Chiti, F. & Dobson, C. M. Protein misfolding, functional amyloid, and human disease. *Annu Rev Biochem* **75**, 333–366 (2006).
2. Zoghbi, H. Y. & Orr, H. T. Glutamine repeats and neurodegeneration. *Annu Rev Neurosci* **23**, 217–247 (2000).
3. Orr, H. T. & Zoghbi, H. Y. Trinucleotide repeat disorders. *Annu Rev Neurosci* **30**, 575–621 (2007).
4. Blum, E. S., Schwendeman, A. R. & Shaham, S. PolyQ disease: misfiring of a developmental cell death program? *Trends Cell Biol* **23**, 168–174 (2013).
5. Perutz, M. F., Johnson, T., Suzuki, M. & Finch, J. T. Glutamine repeats as polar zippers: their possible role in inherited neurodegenerative diseases. *Proc Natl Acad Sci U S A* **91**, 5355–5358 (1994).
6. Chen, S., Ferrone, F. A. & Wetzel, R. Huntington's disease age-of-onset linked to polyglutamine aggregation nucleation. *Proc Natl Acad Sci U S A* **99**, 11884–11889 (2002).
7. Arrasate, M., Mitra, S., Schweitzer, E. S., Segal, M. R. & Finkbeiner, S. Inclusion body formation reduces levels of mutant huntingtin and the risk of neuronal death. *Nature* **431**, 805–810 (2004).
8. Ross, C. A. & Poirier, M. A. Protein aggregation and neurodegenerative disease. *Nat Med* **10 Suppl**, S10–17 (2004).
9. Jiang, Y. J. *et al.* Interaction with polyglutamine-expanded huntingtin alters cellular distribution and RNA processing of huntingtin yeast two-hybrid protein A (HYPA). *J Biol Chem* **286**, 25236–25245 (2011).
10. Olzscha, H. *et al.* Amyloid-like aggregates sequester numerous metastable proteins with essential cellular functions. *Cell* **144**, 67–78 (2011).
11. Qin, Z. H. *et al.* Huntingtin bodies sequester vesicle-associated proteins by a polyproline-dependent interaction. *J Neurosci* **24**, 269–281 (2004).
12. McCampbell, A. *et al.* CREB-binding protein sequestration by expanded polyglutamine. *Hum Mol Genet* **9**, 2197–2202 (2000).
13. Paulson, H. L. *et al.* Intranuclear inclusions of expanded polyglutamine protein in spinocerebellar ataxia type 3. *Neuron* **19**, 333–344 (1997).
14. Park, S. H. *et al.* PolyQ proteins interfere with nuclear degradation of cytosolic proteins by sequestering the Sis1p chaperone. *Cell* **154**, 134–145 (2013).
15. Chai, Y., Shao, J., Miller, V. M., Williams, A. & Paulson, H. L. Live-cell imaging reveals divergent intracellular dynamics of polyglutamine disease proteins and supports a sequestration model of pathogenesis. *Proc Natl Acad Sci U S A* **99**, 9310–9315 (2002).
16. Fujita, K. *et al.* A functional deficiency of TERA/VCP/p97 contributes to impaired DNA repair in multiple polyglutamine diseases. *Nat Commun* **4**, 1816 (2013).
17. Chai, Y., Berke, S. S., Cohen, R. E. & Paulson, H. L. Poly-ubiquitin binding by the polyglutamine disease protein ataxin-3 links its normal function to protein surveillance pathways. *J Biol Chem* **279**, 3605–3611 (2004).
18. Nicastro, G. *et al.* Understanding the role of the Josephin domain in the PolyUb binding and cleavage properties of ataxin-3. *PLoS One* **5**, e12430 (2010).
19. Doss-Pepe, E. W., Stenroos, E. S., Johnson, W. G. & Madura, K. Ataxin-3 interactions with rad23 and valosin-containing protein and its associations with ubiquitin chains and the proteasome are consistent with a role in ubiquitin-mediated proteolysis. *Mol Cell Biol* **23**, 6469–6483 (2003).
20. Wang, Q., Li, L. & Ye, Y. Regulation of retrotranslocation by p97-associated deubiquitinating enzyme ataxin-3. *J Cell Biol* **174**, 963–971 (2006).
21. Zhong, X. & Pittman, R. N. Ataxin-3 binds VCP/p97 and regulates retrotranslocation of ERAD substrates. *Hum Mol Genet* **15**, 2409–2420 (2006).
22. Goto, J. *et al.* Machado-Joseph disease gene products carrying different carboxyl termini. *Neurosci Res* **28**, 373–377 (1997).
23. Berke, S. J., Chai, Y., Marrs, G. L., Wen, H. & Paulson, H. L. Defining the role of ubiquitin-interacting motifs in the polyglutamine disease protein, ataxin-3. *J Biol Chem* **280**, 32026–32034 (2005).
24. Harris, G. M., Dodelzon, K., Gong, L., Gonzalez-Alegre, P. & Paulson, H. L. Splice isoforms of the polyglutamine disease protein ataxin-3 exhibit similar enzymatic yet different aggregation properties. *PLoS One* **5**, e13695 (2010).
25. Song, A. X. *et al.* Structural transformation of the tandem ubiquitin-interacting motifs in ataxin-3 and their cooperative interactions with ubiquitin chains. *PLoS One* **5**, e13202 (2010).
26. Nicastro, G. *et al.* The solution structure of the Josephin domain of ataxin-3: structural determinants for molecular recognition. *Proc Natl Acad Sci U S A* **102**, 10493–10498 (2005).
27. Mao, Y. *et al.* Deubiquitinating function of ataxin-3: insights from the solution structure of the Josephin domain. *Proc Natl Acad Sci U S A* **102**, 12700–12705 (2005).
28. Boeddrich, A. *et al.* An arginine/lysine-rich motif is crucial for VCP/p97-mediated modulation of ataxin-3 fibrillogenesis. *EMBO J* **25**, 1547–1558 (2006).
29. Liu, S., Fu, Q. S., Zhao, J. & Hu, H. Y. Structural and mechanistic insights into the arginine/lysine-rich peptide motifs that interact with P97/VCP. *Biochim Biophys Acta* **1834**, 2672–2678 (2013).
30. Maciel, P. *et al.* Improvement in the molecular diagnosis of Machado-Joseph disease. *Arch Neurol* **58**, 1821–1827 (2001).
31. Seidel, K. *et al.* Axonal inclusions in spinocerebellar ataxia type 3. *Acta Neuropathol* **120**, 449–460 (2010).
32. Hayashi, M., Kobayashi, K. & Furuta, H. Immunohistochemical study of neuronal intranuclear and cytoplasmic inclusions in Machado-Joseph disease. *Psychiatry Clin Neurosci* **57**, 205–213 (2003).
33. Paulson, H. L. *et al.* Machado-Joseph disease gene product is a cytoplasmic protein widely expressed in brain. *Ann Neurol* **41**, 453–462 (1997).
34. Chai, Y., Koppenhafer, S. L., Bonini, N. M. & Paulson, H. L. Analysis of the role of heat shock protein (Hsp) molecular chaperones in polyglutamine disease. *J Neurosci* **19**, 10338–10347 (1999).
35. Chai, Y., Koppenhafer, S. L., Shoesmith, S. J., Perez, M. K. & Paulson, H. L. Evidence for proteasome involvement in polyglutamine disease: localization to nuclear inclusions in SCA3/MJD and suppression of polyglutamine aggregation in vitro. *Hum Mol Genet* **8**, 673–682 (1999).
36. Schmidt, T. *et al.* Protein surveillance machinery in brains with spinocerebellar ataxia type 3: redistribution and differential recruitment of 26S proteasome subunits and chaperones to neuronal intranuclear inclusions. *Ann Neurol* **51**, 302–310 (2002).
37. Mueller, T. *et al.* CK2-dependent phosphorylation determines cellular localization and stability of ataxin-3. *Hum Mol Genet* **18**, 3334–3343 (2009).
38. Breuer, P., Haacke, A., Evert, B. O. & Wullner, U. Nuclear aggregation of polyglutamine-expanded ataxin-3: fragments escape the cytoplasmic quality control. *J Biol Chem* **285**, 6532–6537 (2010).
39. Liu, S. *et al.* NEDD8 ultimate buster-1 long (NUB1L) protein promotes transfer of NEDD8 to proteasome for degradation through the P97UFD1/NPL4 complex. *J Biol Chem* **288**, 31339–31349 (2013).

40. Ferro, A. *et al*. NEDD8: a new ataxin-3 interactor. *Biochim Biophys Acta* **1773**, 1619–1627 (2007).
41. Nicastro, G. *et al*. Josephin domain of ataxin-3 contains two distinct ubiquitin-binding sites. *Biopolymers* **91**, 1203–1214 (2009).
42. Jung, J., Xu, K., Lessing, D. & Bonini, N. M. Preventing Ataxin-3 protein cleavage mitigates degeneration in a Drosophila model of SCA3. *Hum Mol Genet* **18**, 4843–4852 (2009).
43. Goti, D. *et al*. A mutant ataxin-3 putative-cleavage fragment in brains of Machado-Joseph disease patients and transgenic mice is cytotoxic above a critical concentration. *J Neurosci* **24**, 10266–10279 (2004).
44. Masino, L., Nicastro, G., Calder, L., Vendruscolo, M. & Pastore, A. Functional interactions as a survival strategy against abnormal aggregation. *FASEB J* **25**, 45–54 (2011).
45. Davranche, A. *et al*. Huntingtin affinity for partners is not changed by polyglutamine length: aggregation itself triggers aberrant interactions. *Hum Mol Genet* **20**, 2795–2806 (2011).
46. Vachharajani, S. N., Chaudhary, R. K., Prasad, S. & Roy, I. Length of polyglutamine tract affects secondary and tertiary structures of huntingtin protein. *Int J Biol Macromol* **51**, 920–925 (2012).
47. Buchanan, L. E. *et al*. Structural motif of polyglutamine amyloid fibrils discerned with mixed-isotope infrared spectroscopy. *Proc Natl Acad Sci U S A* (2014).
48. Heck, B. S., Doll, F. & Hauser, K. Length-dependent conformational transitions of polyglutamine repeats as molecular origin of fibril initiation. *Biophys Chem* **185**, 47–57 (2014).
49. Frost, B. & Diamond, M. I. Prion-like mechanisms in neurodegenerative diseases. *Nat Rev Neurosci* **11**, 155–159 (2010).
50. Orr, H. T. Cell biology of spinocerebellar ataxia. *J Cell Biol* **197**, 167–177 (2012).
51. Bevivino, A. E. & Loll, P. J. An expanded glutamine repeat destabilizes native ataxin-3 structure and mediates formation of parallel beta -fibrils. *Proc Natl Acad Sci U S A* **98**, 11955–11960 (2001).
52. Nagai, Y. A toxic monomeric conformer of the polyglutamine protein. *Nat Struct Mol Biol* **14**, 332–340 (2007).
53. Chow, M. K., Paulson, H. L. & Bottomley, S. P. Destabilization of a non-pathological variant of ataxin-3 results in fibrillogenesis via a partially folded intermediate: a model for misfolding in polyglutamine disease. *J Mol Biol* **335**, 333–341 (2004).
54. Takahashi, T. *et al*. Soluble polyglutamine oligomers formed prior to inclusion body formation are cytotoxic. *Hum Mol Genet* **17**, 345–356 (2008).
55. Ye, Y., Meyer, H. H. & Rapoport, T. A. The AAA ATPase Cdc48/p97 and its partners transport proteins from the ER into the cytosol. *Nature* **414**, 652–656 (2001).
56. Acs, K. *et al*. The AAA-ATPase VCP/p97 promotes 53BP1 recruitment by removing L3MBTL1 from DNA double-strand breaks. *Nat Struct Mol Biol* **18**, 1345–1350 (2011).
57. Bao, W. J. *et al*. Highly efficient expression and purification system of small-size protein domains in Escherichia coli for biochemical characterization. *Protein Expr Purif* **47**, 599–606 (2006).
58. Raasi, S. & Pickart, C. M. Ubiquitin chain synthesis. *Methods Mol Biol* **301**, 47–55 (2005).
59. Zhang, Y. H., Zhou, C. J., Zhou, Z. R., Song, A. X. & Hu, H. Y. Domain Analysis Reveals That a Deubiquitinating Enzyme USP13 Performs Non-Activating Catalysis for Lys63-Linked Polyubiquitin. *PLoS One* **6**, e29362 (2011).
60. Zhou, Z. R., Zhang, Y. H., Liu, S., Song, A. X. & Hu, H. Y. Length of the active-site crossover loop defines the substrate specificity of ubiquitin C-terminal hydrolases for ubiquitin chains. *Biochem J* **441**, 143–149 (2012).

Author contributions

H.-Y.H., H.Y. and Y.-J.J. designed the research; H.-Y.H. supervised the project; H.Y., S.L., J.-J.L and A.-X.S. performed the biochemical experiments; H.Y., J.-J.L. and A.-X.S. made the plasmids and purified the proteins; J.-J.Li, J.Z. and Y.-J.J. carried out the NMR and ITC experiments and analyzed data.

Additional information

Supplementary information accompanies this paper at http://www.nature.com/scientificreports

Competing financial interests: The authors declare no competing financial interests.

How to cite this article: Yang, H. *et al.* Aggregation of polyglutamine-expanded ataxin-3 sequesters its specific interacting partners into inclusions: Implication in a loss-of-function pathology. *Sci. Rep.* **4**, 6410; DOI:10.1038/srep06410 (2014).